Chemical Science

ROYAL SOCIETY OF CHEMISTRY

EDGE ARTICLE

View Article Online
View Journal | View Issue



Cite this: *Chem. Sci.*, 2021, **12**, 11730

All publication charges for this article have been paid for by the Royal Society of Chemistry

Received 24th June 2021
Accepted 19th July 2021

DOI: 10.1039/d1sc03428f

rsc.li/chemical-science

# Hollow and highly diastereoselective face-rotating polyhedra constructed through rationally engineered facial units†

Xiao Tang,[a] Zhihao Li,[a] Haoliang Liu,[a] Hang Qu,[a] Wenbin Gao,[a] Xue Dong,[a] Shilin Zhang,[a] Xinchang Wang,*[b] Andrew C.-H. Sue,*[a] Liulin Yang,[a] Kai Tan,*[a] Zhongqun Tian[a] and Xiaoyu Cao*[a]

Molecular face-rotating polyhedra (FRP) exhibit complex stereochemistry, rendering it challenging to manipulate their assembly in a stereoselective manner. In our previous work, stereocontrolled FRP were gained at the cost of losing the confined inner space, which hampers their host–guest interactions and potential applications. Through a rational design approach, herein we demonstrate the successful construction of hollow FRP with high diastereoselectivity. Whereas the [4 + 4] imine condensation of *meta*-formyl substituted $C_{3h}$-symmetric **TAT-*m*** and $C_3$-symmetric **Tri-NH$_2$** led to the formation of all feasible FRP-**12** diastereoisomers; the *para*-substituted constitutional isomer, **TAT-*p***, exclusively assembled into a pair of homo-directional enantiomeric FRP-**13**-*CCCC*/*AAAA* with a cavity size larger than 600 Å$^3$. Detailed structural characterizations and theoretical investigations revealed the thermodynamic landscape of FRP assembly can be effectively shaped by modulating the van der Waals repulsive forces among the facial building blocks. Our work provided a novel strategy towards stereospecific assembly of pure organic cages, opening up new opportunities for further applications of these chiral materials.

## Introduction

Rationally designed discrete molecular cages have drawn extensive attention in recent years on account of their wide applications in gas storage,[1] molecular recognition,[2] separation,[1b,3] catalysis,[4] and containment of reactive materials.[5] By fine-tuning the shape, angle or rigidity associated with the molecular building blocks,[6] the geometry and size of the confined space inside the resulting cages can be precisely engineered for specific functions. Introducing handedness into molecular cages further lends a new dimension to asymmetric catalysis[7] and chiral resolution.[8] Nevertheless, manipulating the outcome of cage syntheses, *i.e.* diastereoselectivity, is a challenging task as a result of the minute differences between various diastereoisomers on the thermodynamic landscape. In literature, successful chirality control over coordination-driven assembly can be achieved by regulating the chiral communications among ligands.[9] For instance, by modulating the steric repulsions among ligand edges, Nitschke *et al.* reported the syntheses of a series of metal–organic cages with different degrees of diastereoselectivity.[10] On the other hand, introducing chiral guests may also enable the chirality transfer to the cage hosts, templating the formation of specific diastereoisomers.[11] In both cases, however, the intervention of extra components, *e.g.* metal salts and chiral small molecules, is required. As far as pure organic molecular cages are concerned, examples of stereochemical control through interfacial interactions remain rare.

Recently, our group reported a variety of novel chiral face-rotating polyhedra (FRP)[12] consisting of prochiral 2D facial building blocks, such as truxene (**Tr**)[13] and triazatruxene (**TAT**).[14] The senses of anticlockwise (*A*) or clockwise (*C*) rotations arise when these planar building blocks lose their $\sigma_h$ mirror symmetry upon FRP formation, generating a series of diastereoisomeric cages in the one pot reaction (Fig. S4†). The distribution of the populations of different FRP stereoisomers, instead of being statistically governed, can be biased to favor specific species when interfacial non-covalent interactions are present. For instance, the assembly of **Tr**-based FRP-**2** solely produces the homo-directional *AAAA* cage as a result of the van der Waals repulsion among the interior *n*-butyl side chains (Fig. 1a).[13a] Similarly, the π–π interaction between the **TAT** units

[a]*State Key Laboratory of Physical Chemistry of Solid Surface, Key Laboratory of Chemical Biology of Fujian Province, Collaborative Innovation Center of Chemistry for Energy and Materials (iChEM), College of Chemistry and Chemical Engineering, Xiamen University, Xiamen 361005, P. R. China. E-mail: andrewsue@xmu.edu.cn; ktan@xmu.edu.cn; xcao@xmu.edu.cn*

[b]*School of Electronic Science and Engineering, Xiamen University, Xiamen 361005, P. R. China. E-mail: xcwang@xmu.edu.cn*

† Electronic supplementary information (ESI) available. CCDC 2053589. For ESI and crystallographic data in CIF or other electronic format see DOI: 10.1039/d1sc03428f

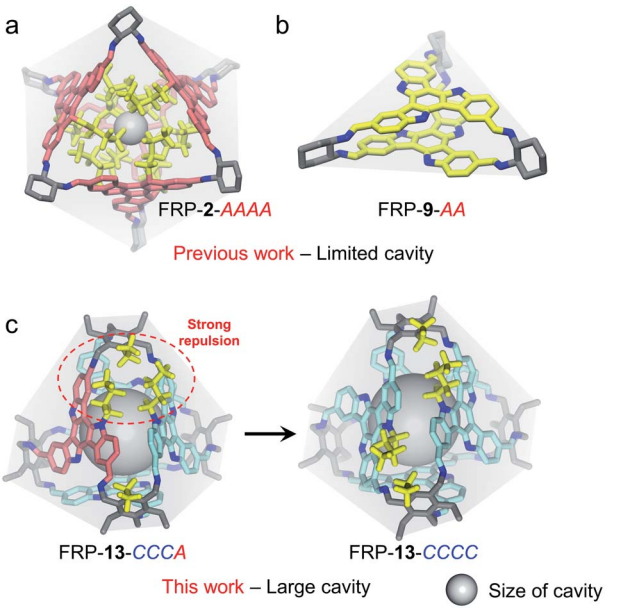


Fig. 1 The van der Waals repulsion (a) and π−π interaction (b) between facial units lead to homo-directional FRP at the cost of inner cavity. (c) The location of facial interaction was moved out of FRP to maintain the cavity size and the strong repulsive force prevented the generation of hetero-directional FRP (*CCCA*/*CAAA* or *CCAA*), resulting in homo-directional FRP-**13**-*CCCC*/*AAAA* with high diastereoselectivity (the *A* and *C* patterns was distinguished by different colour. Part of hydrogen atoms and alkyl chains were omitted for clarity).

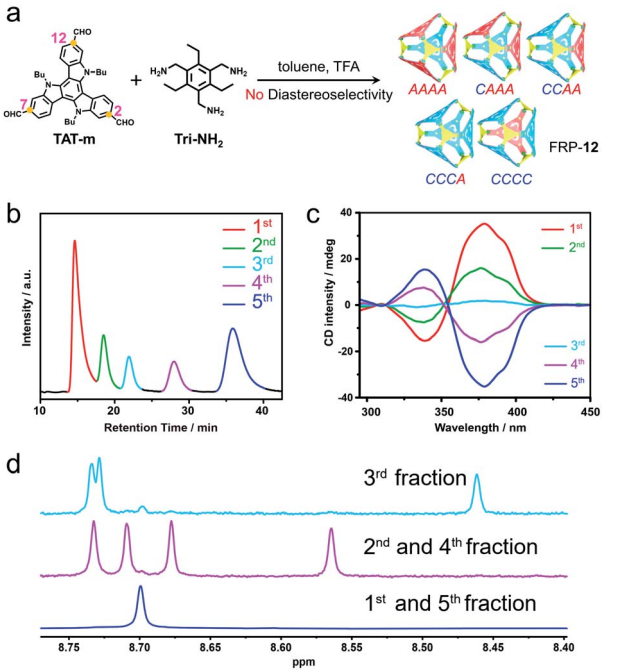


Fig. 2 (a) Non-diastereoselective construction of FRP-**12**. (b) Chiral HPLC analysis showed that FRP-**12** contain five components in 32 : 13 : 10 : 13 : 32 ratios. Detection wavelength: 335 nm. Further characterization confirmed that the configurations of these five fractions of FRP-**12** are *AAAA*, *CAAA*, *CCAA*, *CCCA* and *CCCC* in the order of elution, respectively. (c) CD spectra of all fractions of FRP-**12** recorded in toluene. (d) Partial $^1$H NMR spectra of FRP-**12**. The *T*-(1st and 5th fractions), $C_3$-(2nd and 4th fraction) and $S_4$-(3rd fraction) symmetric polyhedra exhibited one, four and three imine proton peaks, respectively (from bottom to top).

in FRP-**9**-*AA* exclusively leads to the formation of a homo-directional molecular prism (Fig. 1b).[14] Their high diastereoselectivity, nonetheless, was gained at the cost of losing the cavity space of FRP, impeding potential applications in host–guest encapsulation. Herein, we demonstrate the successful construction of a series of [4 + 4] tetrahedral FRP with large inner cavities. In addition, by rationally designing the interfacial interactions between the facial building blocks, these FRP could be tailor-made in a highly diastereroselective fashion (Fig. 1c and S11†).

## Results and discussion

Catalyzed by trifluoroacetic acid (0.075 eq.), the *meta*-formyl substituted **TAT-*m*** (1 eq.) and 1,3,5-triaminomethyl-2,4,6-triethylbenzene (**Tri-NH$_2$**, 1 eq.) were co-assembled into FRP-**12** in toluene through imine condensation reaction[15] (Fig. 2a). High-resolution mass spectrum (HRMS) of FRP-**12** showed a mass-to-charge ratio of 1586.9859, corresponding to [4 + 4] molecular cages composed of four pieces of each building blocks (calculated $m/z$ = 1586.9868 for $[M + 2H]^{2+}$, Fig. S25a†). In theory, five diastereoisomers could stem from different face-rotating patterns on the [4 + 4] tetrahedral FRP-**12**, *i.e.*, homo-directional *AAAA*/*CCCC*, and hetero-directional *CAAA*/*CCCA* and *CCAA* (Fig. 2a and S11†). This is in perfect agreement with the fact that five distinct fractions of FRP-**12** were resolved by employing high-performance liquid chromatography (HPLC) with a chiral stationary phase, respectively eluting at 14.3, 17.7, 21.4, 27.3 and 31.0 min. Preliminary assignments of these fractions can be made based on the averaged symmetry reflected in their $^1$H-NMR spectra.[10,13a] With only a single set of imine proton signals observed, the 1st/5th fractions collected were designated as the FRP-**12**-*AAAA*/*CCCC* isomers, which possess the highest *T*-symmetry. Similarly, the 2nd/4th and the 3rd fractions could be identified as the $C_3$-symmetric FRP-**12**-*CAAA*/*CCCA* and $S_4$-symmetric FRP-**12**-*CCAA* isomers, respectively (Fig. 2d and S4b†). The absolute configurations of FRP-**12** were further determined based on the comparisons between the experimental and (ZINDO/S)-calculated CD spectra. By relating the magnitudes of the Cotton effects to the facial patterns (Fig. 2c and S28†),[14] these five fractions were assigned as FRP-**12**-*AAAA*, *CAAA*, *CCAA*, *CCCA* and *CCCC* in the order of their elution time.

The assembly of FRP-**12** gave rise to a complicated mixture of stereoisomeric molecular cages, whose non-trivial chiral separation inevitably impeded their further developments in both research and practical applications. In our previous work, it was shown that employing different **TAT** constitutional isomers as building blocks of FRP led to totally distinct geometry and diastereoselectivity.[14] Inspired by the significant impact of molecular design on the FRP assembly processes, we produced the *in silico* structures of FRP-**12** (Fig. S32†), as well as a new

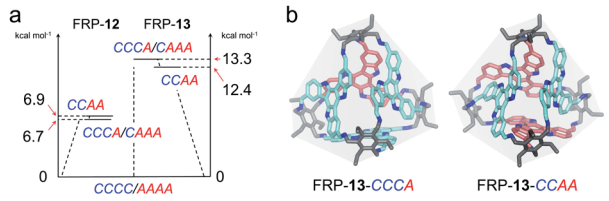


Fig. 3 (a) Computationally optimized structures of FRP-**12** and FRP-**13** series show distinct energy profiles. The hetero-directional FRP-**12**-*CCAA* and *CCCA*/*CAAA* were found to be 6.9 and 6.7 kcal mol$^{-1}$ less stable than the of homo-directional FRP-**12**-*CCCC*/*AAAA* analogues, respectively. On the other hand, the energy gaps between homo- and hetero-directional FRP-**13** were estimated to be larger at 12.4 and 13.3 kcal mol$^{-1}$, respectively. (b) The optimized structures of FRP-**13**-*CCCA* (left) and *CCAA* (right) (hydrogen atoms and the *n*-alkyl chains were omitted for clarity).

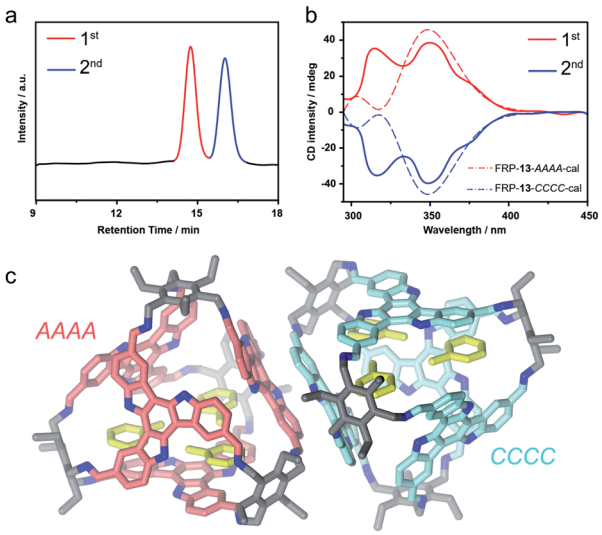


Fig. 4 (a) Chiral HPLC analysis revealed that FRP-**13** are consisted of two components in 1 : 1 ratio. Detection wavelength: 335 nm. Further characterizations confirmed that the directionality of the first and second fractions of FRP-**13** are *AAAA* and *CCCC*, respectively. (b) Experimental and calculated (dash line) CD spectra of FRP-**13** recorded in toluene. (c) Crystal structures of FRP-**13**-*AAAA* and *CCCC*. The toluene molecules inside the FRP are emphasized in yellow (hydrogen atoms and the *n*-alkyl chains were omitted for clarity).

series of FRP-**13** involving *para*-formyl substituted **TAT-*p*** facial units instead of **TAT-*m***. The calculations of the relative energy levels of different diastereoisomers in both series of FRP were performed on Vienna *Ab initio* Simulation Package (VASP), using gradient corrected (PBE) density functional theory in vacuum with D3-BJ dispersion correction. In the case of FRP-**12**, the hetero-directional *CCAA* and *CCCA*/*CAAA* isomers were found to be 6–7 kcal mol$^{-1}$ slightly less stable than their homo-directional *CCCC*/*AAAA* analogues (Fig. 3a, left). In contrast, the energy gaps between the most stable FRP-**13**-*CCCC*/*AAAA* enantiomeric pair and the hetero-directional isomers, namely FRP-**13**-*CCCA*/*CAAA* and *CCAA*, were predicted to be wider at 12–13 kcal mol$^{-1}$ (Fig. 3a, right).

FRP-**13** *in vitro* were assembled from the *para*-formyl substituted **TAT-*p*** facial building blocks and the **Tri-NH$_2$** vertexes with a recipe similar to that of FRP-**12**. All structural characterizations were also carried out by following the routine. The [4 + 4] molecular topology was confirmed by HRMS (Fig. 1c and S25b†). The high symmetry of FRP-**13**, as revealed by the simple pattern featured in the $^1$H NMR spectra, corroborates the *T*-symmetric homo-directional *CCCC*/*AAAA* isomers (Fig. S20–S24†). The chiral HPLC analysis also showed coherent results that FRP-**13** could be successfully resolved into two fractions showing antipodal CD spectra (Fig. 4a and b). The 2nd fraction exhibited a negative Cotton effect at circa 350 nm, corresponding to the calculated FRP-**13**-*CCCC* (Fig. 4b and S31†), and the 1st peak was then assigned as FRP-**13**-*AAAA* accordingly.

In addition, single crystals of FRP-**13** were cured by slowly diffusing methanol into a toluene solution. Unambiguous structural elucidation was enabled by X-ray crystallography, revealing a pair of enantiomeric FRP-**13**-*CCCC*/*AAAA* tetrahedral cages were co-crystalized in $R\bar{3}c$ space group (Fig. 4c). Interestingly, although FRP-**13** shows a time-averaged *T*-symmetry in solution, in the crystal structure one of the **TAT** facial units shifts closer to the centroid of the cage, making the solid-state conformation of FRP-**13** $C_3$-symmetric, presumably as a result of more efficient packing (Fig. S37 and S38†). Moreover, three toluene solvent molecules can be found inside of the cavity, indicating the potential for host–guest interactions. The cavity volume of FRP-**13**-*CCCC*/*AAAA* is estimated to be 772 Å$^3$ by promolecular density (the cavity volume can also be calculated to be 609 Å$^3$ according to the radius of its inscribed sphere, see in Fig. S39 and S40†). In agreement with the theoretically calculated energy levels, the experimental results of NMR, HPLC, CD and single crystal structures unanimously suggested that *para*-substituted **TAT-*p*** underwent highly diastereoselective assembly process with **Tri-NH$_2$** to form a pair of homo-directional enantiomeric cages out of five possible diastereoisomers.

Further structural analysis showed that the two types of facial building blocks, **TAT-*m*** and **TAT-*p***, when assembled with **Tri-NH$_2$**, cause a ~22° difference in the facial rotational angle in the resulting FRP (Fig. S36†). This minor structural variation, coupled with the multifaceted face-rotating patterns, leads to distinct spatial arrangements of their *n*-butyl chains. For both FRP-**12** and **13**-*CCCC*/*AAAA*, the bulky *n*-butyl groups between their **TAT** faces are placed far off from each other and show little steric repulsion (Fig. S33a and c†), which is in accordance with the fact that experimentally the homo-directional stereoisomers are the most stable species obtained.

Similarly, relative weak steric interactions are expected for the hetero-directional FRP-**12**-*CCCA*/*AAAC* or *CCAA*, as their *n*-butyl side chains are positioned away from the **Tri-NH$_2$** vertexes in the molecular models (Fig. 5a and S33d†). The non-covalent interactions among the building blocks, which could be visualized with the aid of reduced density gradient (RDG) analysis,[16] confirmed that only low-density and low-gradient regions exist between the hetero-directional **TAT-*m*** faces (Fig. 5a, right). On the other hand, in hetero-directional FRP-**13**-*CCCA*/*AAAC* and *CCAA* isomers, the alkyl chains between the facial units are

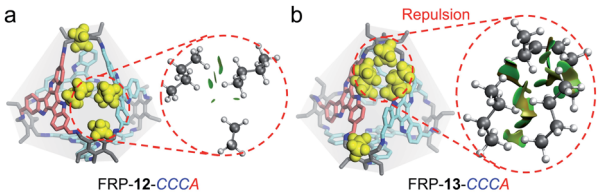


Fig. 5 Computationally optimized structures of FRP-**12**-*CCCA* (a) and FRP-**13**-*CCCA* (b). The alkyl groups between hetero-directional **TAT** units are highlighted in yellow. The RDG analysis indicates that the repulsive interactions between hetero-directional **TAT** units in FRP-**13**-*CCCA* (right) are much stronger than that in FRP-**12**-*CCCA* (left) (hydrogen atoms on the FRP backbone were omitted for clarity).

located much closer to the ethyl groups of **Tri-NH$_2$** vertexes (Fig. 5b and S33b†). The strong repulsive interactions between the hetero-directional **TAT-*p*** units of FRP-**13**-*CCCA* can be clearly manifested by the RDG isosurface (Fig. 5b, right). The crowding of the imine bond protons and **Tri-NH$_2$** units, as identified by RDG analysis (Fig. S34 and S35†), also makes the formations of the hetero-directional FRP-**13** highly unfavored, leaving the FRP-**13**-*CCCC*/*AAAA* as the sole thermodynamic products.

## Conclusions

In conclusion, we have successfully constructed two novel series of hollow [4 + 4] face-rotating polyhedral, FRP-**12** and **13**, with various degree of diastereoselectivity and large cavity. Structural characterizations and theoretical calculations indicated that the effective interfacial interactions between the **TAT** building blocks are essential to the outcome of the cage assembly processes. Whereas the condensation of *meta*-substituted **TAT-*m*** facial building blocks with **Tri-NH$_2$** vertexes formed a mixture of five FRP-**12** stereoisomers, moving the formyl group on the facial units to the *para*-positions completely changed the picture. The minor structural tweaking resulted in ~22° rotations of all facial units in FRP-**13**, bringing out clashing alkyl–alkyl interactions between **TAT-*p*** units, as well as the unfavored gauche conformations of the imine linkages, in the FRP with hetero-directional configurations. On account of the large energy gaps between the hetero- and homo-directional diastereoisomers, FRP-**13** were obtained as a pair of *CCCC*/*AAAA* enantiomers exclusively. The highly diastereo-selective assembly of FRP-**13** provides an example of stereo-controlled construction of pure organic cages by rational molecular design. This work clearly revealed the mechanism for the generation of highly diastereoselective FRP with large inner voids, opening up future opportunities for the constructions of more diverse optically-pure FRP and the further research in chiral resolution, asymmetric catalysis and bio-recognition applications.

## Data availability

All associated computational and experimental details are provided in the ESI.†

## Author contributions

X.-Y. Cao, X.-C. Wang, X. Tang and Andrew C.-H. Sue conceived, initiated and developed this work. X. Tang synthesized the face-rotating polyhedra and participated in all the data analysis. K. Tan and Z.-H. Li performed the theoretical calculation and RDG analysis. H.-L. Liu and S.-L. Zhang carried out the chiral HPLC and CD analysis. Z.-H. Li and W.-B. Gao performed the MS and NMR characterizations. X. Dong and W.-B. Gao characterized the structure of single crystal. X. Tang and Andrew C.-H. Sue drafted the manuscript with contributions from K. Tan, X.-C. Wang, H. Qu, L.-L. Yang, Z.-Q. Tian and X.-Y. Cao. All authors discussed the results and commented on the manuscript.

## Conflicts of interest

There are no conflicts to declare.

## Acknowledgements

We thank Pei Zhang, Yu Wang, Zhiwei Lin, Liubin Feng, Hongxun Fang, Changqing Rao, Si Chen and Xujing Lin for helpful discussion and assistance in experiments. This work was supported by the National Natural Science Foundation of China (NSFC) (No. 21971216, 21722304, 91427304, 21573181 and 91227111), the Top-Notch Young Talents Program of China and the Fundamental Research Funds for the Central Universities of China (No. 20720160050).

## References

1 (*a*) T. Hasell, J. A. Armstrong, K. E. Jelfs, F. H. Tay, K. M. Thomas, S. G. Kazarian and A. I. Cooper, *Chem. Commun.*, 2013, **49**, 9410–9412; (*b*) L. J. Chen, P. S. Reiss, S. Y. Chong, D. Holden, K. E. Jelfs, T. Hasell, M. A. Little, A. Kewley, M. E. Briggs, A. Stephenson, K. M. Thomas, J. A. Armstrong, J. Bell, J. Busto, R. Noel, J. Liu, D. M. Strachan, P. K. Thallapally and A. I. Cooper, *Nat. Mater.*, 2014, **13**, 954–960; (*c*) G. Zhang, O. Presly, F. White, I. M. Oppel and M. Mastalerz, *Angew. Chem., Int. Ed.*, 2014, **53**, 1516–1520.

2 (*a*) C. X. Zhang, Q. Wang, H. Long and W. Zhang, *J. Am. Chem. Soc.*, 2011, **133**, 20995–21001; (*b*) C. X. Zhang, H. Long and W. Zhang, *Chem. Commun.*, 2012, **48**, 6172–6174; (*c*) L. Zhao, Y. L. Chu, C. He and C. Y. Duan, *Chem. Commun.*, 2014, **50**, 3467–3469; (*d*) W. M. Bloch, Y. Abe, J. J. Holstein, C. M. Wandtke, B. Dittrich and G. H. Clever, *J. Am. Chem. Soc.*, 2016, **138**, 13750–13755; (*e*) M. M. Zhang, M. L. Saha, M. Wang, Z. X. Zhou, B. Song, C. J. Lu, X. Z. Yan, X. P. Li, F. H. Huang, S. C. Yin and P. J. Stang, *J. Am. Chem. Soc.*, 2017, **139**, 5067–5074; (*f*) W. Y. Zhang, D. Yang, J. Zhao, L. K. Hou, J. L. Sessler, X. J. Yang and B. Wu, *J. Am. Chem. Soc.*, 2018, **140**, 5248–5256; (*g*) R. J. Li, J. J. Holstein, W. G. Hiller, J. Andréasson and G. H. Clever, *J. Am. Chem. Soc.*, 2019, **141**, 2097–2103; (*h*) L. Zhang, Y. Jin, G.-H. Tao, Y. Gong, Y. Hu, L. He and W. Zhang, *Angew. Chem., Int. Ed.*, 2020, **59**, 20846–20851.

3 T. Mitra, K. E. Jelfs, M. Schmidtmann, A. Ahmed, S. Y. Chong, D. J. Adams and A. I. Cooper, *Nat. Chem.*, 2013, **5**, 276–281.

4 (*a*) M. Yoshizawa, M. Tamura and M. Fujita, *Science*, 2006, **312**, 251–254; (*b*) M. D. Pluth, R. G. Bergman and K. N. Raymond, *Science*, 2007, **316**, 85–88; (*c*) C. J. Hastings, D. Fiedler, R. G. Bergman and K. N. Raymond, *J. Am. Chem. Soc.*, 2008, **130**, 10977–10983; (*d*) W. Cullen, M. C. Misuraca, C. A. Hunter, N. H. Williams and M. D. Ward, *Nat. Chem.*, 2016, **8**, 231–236; (*e*) L. Qiu, R. McCaffrey, Y. Jin, Y. Gong, Y. Hu, H. Sun, W. Park and W. Zhang, *Chem. Sci.*, 2018, **9**, 676–680; (*f*) N. Sun, C. Wang, H. Wang, L. Yang, P. Jin, W. Zhang and J. Jiang, *Angew. Chem., Int. Ed.*, 2019, **58**, 18011–18016.

5 (*a*) P. Mal, B. Breiner, K. Rissanen and J. R. Nitschke, *Science*, 2009, **324**, 1697–1699; (*b*) T. Y. Jiao, L. Chen, D. Yang, X. Li, G. C. Wu, P. M. Zeng, A. K. Zhou, Q. Yin, Y. J. Pan, B. Wu, X. Hong, X. Q. Kong, V. M. Lynch, J. L. Sessler and H. Li, *Angew. Chem., Int. Ed.*, 2017, **56**, 14545–14550; (*c*) D. Yang, J. Zhao, L. Yu, X. Lin, W. Zhang, H. Ma, A. Gogoll, Z. Zhang, Y. Wang, X. J. Yang and B. Wu, *J. Am. Chem. Soc.*, 2017, **139**, 5946–5951.

6 (*a*) M. Fujita, S. Nagao and K. Ogura, *J. Am. Chem. Soc.*, 1995, **117**, 1649–1650; (*b*) M. Mastalerz, *Chem. Commun.*, 2008, 4756–4758; (*c*) T. Hasell, X. F. Wu, J. T. Jones, J. Bacsa, A. Steiner, T. Mitra, A. Trewin, D. J. Adams and A. I. Cooper, *Nat. Chem.*, 2010, **2**, 750–755; (*d*) Q. F. Sun, J. Iwasa, D. Ogawa, Y. Ishido, S. Sato, T. Ozeki, Y. Sei, K. Yamaguchi and M. Fujita, *Science*, 2010, **328**, 1144–1147; (*e*) Y. Z. Liu, C. H. Hu, A. Comotti and M. D. Ward, *Science*, 2011, **333**, 436–440; (*f*) H. Li, H. C. Zhang, A. D. Lammer, M. Wang, X. P. Li, V. M. Lynch and J. L. Sessler, *Nat. Chem.*, 2015, **7**, 1003–1008; (*g*) S. Zarra, D. M. Wood, D. A. Roberts and J. R. Nitschke, *Chem. Soc. Rev.*, 2015, **44**, 419–432; (*h*) T. R. Cook and P. J. Stang, *Chem. Rev.*, 2015, **115**, 7001–7045; (*i*) D. Fujita, Y. Ueda, S. Sato, N. Mizuno, T. Kumasaka and M. Fujita, *Nature*, 2016, **540**, 563–566; (*j*) S. Chakraborty, W. Hong, K. J. Endres, T. Z. Xie, L. Wojtas, C. N. Moorefield, C. Wesdemiotis and G. R. Newkome, *J. Am. Chem. Soc.*, 2017, **139**, 3012–3020; (*k*) B. Chen, J. J. Holstein, S. Horiuchi, W. G. Hiller and G. H. Clever, *J. Am. Chem. Soc.*, 2019, **141**, 8907–8913; (*l*) S. Huang, Z. Lei, Y. Jin and W. Zhang, *Chem. Sci.*, 2021, **12**, 9591–9606.

7 (*a*) C. Zhao, Q. F. Sun, W. M. Hart-Cooper, A. G. DiPasquale, F. D. Toste, R. G. Bergman and K. N. Raymond, *J. Am. Chem. Soc.*, 2013, **135**, 18802–18805; (*b*) J. Guo, Y. W. Xu, K. Li, L. M. Xiao, S. Chen, K. Wu, X. D. Chen, Y. Z. Fan, J. M. Liu and C. Y. Su, *Angew. Chem., Int. Ed.*, 2017, **56**, 3852–3856; (*c*) J. J. Jiao, C. X. Tan, Z. J. Li, Y. Liu, X. Han and Y. Cui, *J. Am. Chem. Soc.*, 2018, **140**, 2251–2259; (*d*) C. X. Tan, J. J. Jiao, Z. J. Li, Y. Liu, X. Han and Y. Cui, *Angew. Chem., Int. Ed.*, 2018, **57**, 2085–2090; (*e*) C. X. Tan, D. D. Chu, X. H. Tang, Y. Liu, W. M. Xuan and Y. Cui, *Chem.–Eur. J.*, 2019, **25**, 662–672; (*f*) Y. Wang, Y. B. Sun, P. C. Shi, M. M. Sartin, X. J. Lin, P. Zhang, H. X. Fang, P. X. Peng, Z. Q. Tian and X. Y. Cao, *Chem. Sci.*, 2019, **10**, 8076–8082; (*g*) P. M. Punt, M. D. Langenberg, O. Altan and G. H. Clever, *J. Am. Chem. Soc.*, 2021, **143**, 3555–3561.

8 (*a*) W. M. Xuan, M. N. Zhang, Y. Liu, Z. J. Chen and Y. Cui, *J. Am. Chem. Soc.*, 2012, **134**, 6904–6907; (*b*) K. Wu, K. Li, Y. J. Hou, M. Pan, L. Y. Zhang, L. Chen and C. Y. Su, *Nat. Commun.*, 2016, **7**, 10487; (*c*) Y. J. Hou, K. Wu, Z. W. Wei, K. Li, Y. L. Lu, C. Y. Zhu, J. S. Wang, M. Pan, J. J. Jiang, G. Q. Li and C. Y. Su, *J. Am. Chem. Soc.*, 2018, **140**, 18183–18191.

9 (*a*) N. Ousaka, J. K. Clegg and J. R. Nitschke, *Angew. Chem., Int. Ed.*, 2012, **51**, 1464–1468; (*b*) M. C. Young, L. R. Holloway, A. M. Johnson and R. J. Hooley, *Angew. Chem., Int. Ed.*, 2014, **53**, 9832–9836; (*c*) L. L. Yan, C. H. Tan, G. L. Zhang, L. P. Zhou, J. C. Bunzli and Q. F. Sun, *J. Am. Chem. Soc.*, 2015, **137**, 8550–8555; (*d*) A. M. Castilla, M. A. Miller, J. R. Nitschke and M. M. Smulders, *Angew. Chem., Int. Ed.*, 2016, **55**, 10616–10620; (*e*) Y. Y. Zhou, H. F. Li, T. Y. Zhu, T. Gao and P. F. Yan, *J. Am. Chem. Soc.*, 2019, **141**, 19634–19643; (*f*) P. Howlader, E. Zangrando and P. S. Mukherjee, *J. Am. Chem. Soc.*, 2020, **142**, 9070–9078; (*g*) Q. X. Shi, X. H. Zhou, W. Yuan, X. S. Su, A. Neniskis, X. Wei, L. Taujenis, G. Snarskis, J. S. Ward, K. Rissanen, J. de Mendoza and E. Orentas, *J. Am. Chem. Soc.*, 2020, **142**, 3658–3670.

10 W. J. Meng, J. K. Clegg, J. D. Thoburn and J. R. Nitschke, *J. Am. Chem. Soc.*, 2011, **133**, 13652–13660.

11 (*a*) C. M. Hong, D. M. Kaphan, R. G. Bergman, K. N. Raymond and F. D. Toste, *J. Am. Chem. Soc.*, 2017, **139**, 8013–8021; (*b*) D. W. Zhang, T. K. Ronson, J. L. Greenfield, T. Brotin, P. Berthault, E. Leonce, J. L. Zhu, L. Xu and J. R. Nitschke, *J. Am. Chem. Soc.*, 2019, **141**, 8339–8345; (*c*) C. Bravin, G. Mason, G. Licini and C. Zonta, *J. Am. Chem. Soc.*, 2019, **141**, 11963–11969; (*d*) P. Howlader, S. Mondal, S. Ahmed and P. S. Mukherjee, *J. Am. Chem. Soc.*, 2020, **142**, 20968–20972; (*e*) L. Cheng, K. Liu, Y. J. Duan, H. H. Duan, Y. W. Li, M. Gao and L. P. Cao, *CCS Chem.*, 2020, 2749–2751; (*f*) B. Y. Li, B. Zheng, W. Y. Zhang, D. Zhang, X. J. Yang and B. Wu, *J. Am. Chem. Soc.*, 2020, **142**, 6304–6311.

12 (*a*) R. B. Fuller, A. L. Loeb and E. J. Applewhtie, *Synergetics: Explorations in the Geometry of Thinking*, Macmillan Pub. Co., 1975; (*b*) Y. Wang, H. X. Fang, W. Zhang, Y. B. Zhuang, Z. Q. Tian and X. Y. Cao, *Chem. Commun.*, 2017, **53**, 8956–8959; (*c*) H. Qu, Z. Y. Huang, X. Dong, X. C. Wang, X. Tang, Z. H. Li, W. B. Gao, H. L. Liu, R. S. Huang, Z. J. Zhao, H. Zhang, L. L. Yang, Z. Q. Tian and X. Y. Cao, *J. Am. Chem. Soc.*, 2020, **142**, 16223–16228.

13 (*a*) X. C. Wang, Y. Wang, H. Y. Yang, H. X. Fang, R. Chen, Y. B. Sun, N. F. Zheng, K. Tan, X. Lu, Z. Q. Tian and X. Y. Cao, *Nat. Commun.*, 2016, **7**, 12469; (*b*) Y. Wang, H. X. Fang, I. Tranca, H. Qu, X. C. Wang, A. J. Markvoort, Z. Q. Tian and X. Y. Cao, *Nat. Commun.*, 2018, **9**, 488.

14 P. Zhang, X. C. Wang, W. Xuan, P. X. Peng, Z. H. Li, R. Q. Lu, S. Wu, Z. Q. Tian and X. Y. Cao, *Chem. Commun.*, 2018, **54**, 4685–4688.

15 (*a*) M. E. Belowich and J. F. Stoddart, *Chem. Soc. Rev.*, 2012, **41**, 2003–2024; (*b*) Y. H. Jin, Q. Wang, P. Taynton and W. Zhang, *Acc. Chem. Res.*, 2014, **47**, 1575–1586.

16 E. R. Johnson, S. Keinan, P. Mori-Sanchez, J. Contreras-Garcia, A. J. Cohen and W. T. Yang, *J. Am. Chem. Soc.*, 2010, **132**, 6498–6506.